

## Seismic performance of isolated curved steel viaducts under level II earthquakes

Carlos Mendez Galindo \*, Toshiro Hayashikawa \*\* and Daniel Ruiz Julian \*\*\*

\* Graduate Student, Graduate School of Eng., Hokkaido University, Nishi 8 Kita 13 Kita-ku, Sapporo 060-8628

\*\* Dr. of Eng., Professor, Graduate School of Eng., Hokkaido University, Nishi 8 Kita 13 Kita-ku, Sapporo 060-8628

\*\*\* Former Graduate Student, Graduate School of Eng., Hokkaido University, Nishi 8 Kita 13 Kita-ku, Sapporo 060-8628

This paper investigates the effectiveness of the use of seismic isolation devices on the overall 3D seismic response of curved highway viaducts with an emphasis on expansion joints. Furthermore, an evaluation of the effectiveness of the use of cable restrainers is presented. For this purpose, the bridge seismic performance has been evaluated on four different radii of curvature, considering two cases: restrained and unrestrained curved viaducts. Depending on the radius of curvature, three-dimensional non-linear dynamic analysis shows the vulnerability of curved viaducts to pounding and deck unseating damage. In this study, the efficiency of using LRB supports combined with cable restrainers on curved viaducts is demonstrated, not only by reducing in all cases the possible damage, but also by providing a similar behavior in the viaducts despite of curvature radius.

*Keywords: Nonlinear dynamic response, unseating prevention system, seismic design*

### 1. INTRODUCTION

In recent years, horizontally curved steel viaducts have become an important component in modern highway systems as the most viable option at complicated interchanges or river crossings where geometric restrictions and constraints of limited site space make extremely complicated the adoption of standard straight superstructures.

Curved alignments offer, in addition, the benefits of aesthetically pleasing, traffic sight distance increase, as well as economically competitive construction costs with regard to straight bridges. On the contrary, steel viaducts with curved configurations may sustain severe seismic damage owing to rotation of the superstructure or displacement toward the outside of the curve line due to complex vibrations occurring during strong earthquake ground motions<sup>1)</sup>.

The South Fork Eel River Bridge, a curved steel girder bridge located 49 km from the epicenter of the 1992 Petrolia earthquake, sustained considerable damage at hinge locations with a large impact on its service capacity. The partial collapse during the 1994 Northridge earthquake of two curved bridges at the Interstate 5 and State Road 14 interchange is another example to corroborate the seismic vulnerability of curved bridge structures during past earthquakes.

During history, severe strong earthquakes have repeatedly demonstrated that during an earthquake, adjacent spans often vibrate out-of-phase, causing two different types of displacement problems. The first type is a localized damage caused by the spans pounding together at the joints. The second type occurs when the expansion joint separates, possibly allowing the deck superstructure to become unseated from the supporting substructure if the seismically induced displacements are excessively large. Additionally, bridges with curved configurations may sustain severe damage owing to rotation of the superstructure or displacement toward the outside of the curve line during an earthquake<sup>1)</sup>. For this reason, curved bridges have suffered severe damage in past earthquakes.

The implementation of modern seismic protection technologies has permitted the seismic modernization of bridges through the installation of cable restrainers that provide connection between adjacent spans. The purpose is to prevent the unseating of decks from top of the piers at expansion joints by limiting the relative movements of adjacent bridge superstructures. Moreover, cable restrainers provide a fail-safe function by supporting a fallen girder unseated in the event of a severe earthquake<sup>1)</sup>. In addition, another commonly adopted earthquake protection strategy consists of replacing the vulnerable steel bearing supports with seismic isolation devices.

Among the great variety of seismic isolation systems, lead-rubber bearing (LRB) has found wide application in bridge structures. This is due to its simplicity and the combined isolation-energy dissipation function in a single compact unit. Even though the application of the mentioned earthquake protection techniques, the considerable complexity associated with the analysis of curved viaducts requires a realistic prediction of the structural response, especially under the extreme ground motions generated by Level II earthquakes. The effect of the curvature plays also an important role in the seismic behavior of curved highway viaducts, by increasing the bridge vulnerabilities during an earthquake<sup>2)</sup>.

Based on the above considerations, it is clear how the necessity of an accurate design of new bridges and the seismic evaluation of existing structures have become deeply felt issues. It is broadly recognized that curved bridges are complex and unique structures, which can be subjected to different vibration movements during an earthquake. Consequently, a realistic prediction of the bridge seismic response should consider the adoption of refined three-dimensional finite-element models. While the use of isolators combined with cable restrainers have been widely studied on straight bridges, there is still a necessity of more accurate studies for curved viaducts, particularly regarding the effect of the curvature radius.

Therefore, the purpose of the present study is to analyze the overall performance of seismically isolated highway viaducts with different radii of curvature. The effect of curvature on deck unseating damage and pounding damage is analyzed. In addition, a comparison between restrained and unrestrained highway bridges is presented. The study combines the use of non-linear dynamic analysis with a three-dimensional bridge model to accurately evaluate the seismic demands on four radii of curvature in the event of severe earthquakes.

## 2. ANALYTICAL MODEL OF VIADUCTS

The great complexness related to the seismic analysis of highway viaducts enhances a realistic prediction of the bridge structural responses. This fact provides a valuable environment for the non-linear behavior due to material and geometrical non-linearities of the relatively large deflection of the structure on the stresses and forces. Therefore, the seismic analysis of the viaduct employs non-linear computer model that simulates the highly non-linear response due to impacts at the expansion joints. Non-linearities are also considered for characterization of the non-linear structural elements of piers, bearings and cable restrainers.

The highway viaduct considered in the analysis is composed by a three-span continuous section connected to a single simply supported span. The overall viaduct length of 160 m is divided in equal spans of 40 m, as represented in Fig. 1-a. The bridge alignment is horizontally curved in a circular arc. Four different

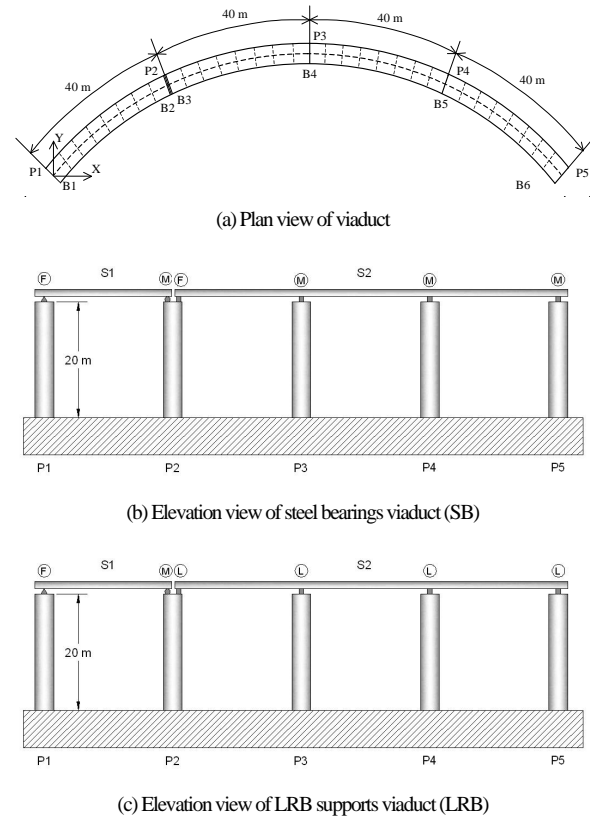


**Fig. 1** Model of curved highway viaduct

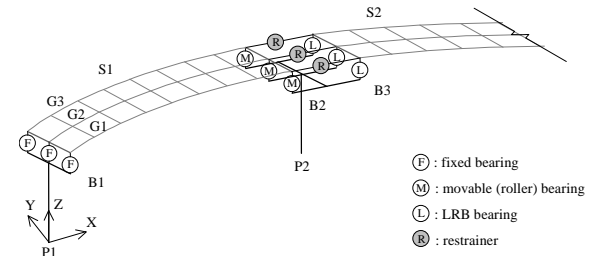


**Fig. 2** Detail of curved viaduct finite element model

radii of curvature are taken into consideration measured from the origin of the circular arc to the centerline of the bridge deck. Tangential configuration for both piers and bearing supports is adopted, respect to the global coordinate system for the bridge, shown in the figure, in which the X- and Y-axes lie in the horizontal plane while the Z-axis is vertical.

### 2.1 Deck Superstructure and Piers

The bridge superstructure consists of a concrete deck slab that rests on three I-shape steel girders, equally spaced at an interval of 2.1 m. The girders are interconnected by end-span diaphragms as well as intermediate diaphragms at uniform spacing of 5.0 m. Full composite action between the slab and the girders is assumed for the superstructure model, which is treated as a three-dimensional grillage beam system shown in

**Table 1** Cross sectional properties of deck and piers

|    | $A \text{ (m}^2\text{)}$ | $I_x \text{ (m}^4\text{)}$ | $I_y \text{ (m}^4\text{)}^{(1)}$ |
|----|--------------------------|----------------------------|----------------------------------|
| P1 | 0.4500                   | 0.3798                     | 0.3798                           |
| P2 | 0.4700                   | 0.4329                     | 0.4329                           |
| P3 | 0.4700                   | 0.4329                     | 0.4329                           |
| P4 | 0.4700                   | 0.4329                     | 0.4329                           |
| P5 | 0.4500                   | 0.3798                     | 0.3798                           |
| G1 | 0.2100                   | 0.1005                     | 0.0994                           |
| G2 | 0.4200                   | 0.1609                     | 0.2182                           |
| G3 | 0.2100                   | 0.1005                     | 0.0994                           |

<sup>(1)</sup>  $I_z$  in case of G1, G2 and G3

**Table 2** Structural properties of LRB supports

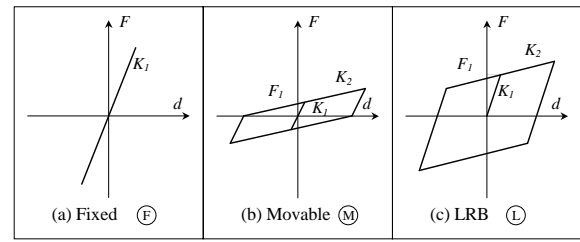
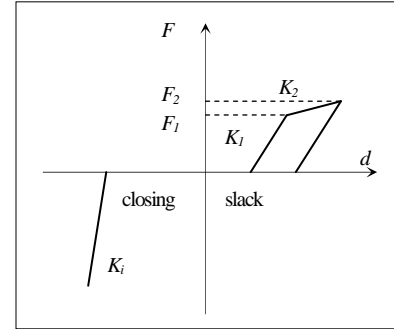
| Pier Location | $K_1$<br>(MN/m) | $K_2$<br>(MN/m) | $F_l$<br>(MN) |
|---------------|-----------------|-----------------|---------------|
| P3, P4        | 49.00           | 4.90            | 0.490         |
| P2, P5        | 36.75           | 3.68            | 0.368         |

Fig. 2. The deck weight is supported on five hollow box section steel piers of 20m height designed according to the seismic code in Japan<sup>1)</sup>. Two cases have been considered, the first case in which the superstructure is supported on steel bearings (SB), and the second in which the continuous section has been seismically isolated (LRB), as is shown in Figs. 1-b and 1-c. Cross sectional properties of the deck and the bridge piers are summarized in Table 1. Densities of steel and concrete are 7850 kg/m<sup>3</sup> and 2500 kg/m<sup>3</sup>, respectively.

Characterization of structural pier elements is based on the fiber element modelization where the inelasticity of the flexure element is accounted by the division of the cross-section into a discrete number of longitudinal and transversal fiber regions with constitutive model based on uniaxial stress-strain relationship for each zone. The element stress resultants are determined by integration of the fiber zone stresses over the cross section of the element. At the pier locations the viaduct deck is modeled in the transverse direction as a rigid bar of length equal to the deck width. This transverse rigid bar is used to model the interactions between deck and pier motions<sup>3)</sup>.

## 2.2 Bearing Supports

In both cases, SB and LRB, steel fixed bearing supports (shown in Fig. 3-a) are installed across the full width on the left end of the simply-supported span (S1), resting on the Pier 1 (P1). Steel roller bearings at the right end on the Pier 2 (P2) allow for movement in the longitudinal (tangent to the curved superstructure) direction while restrained in the transverse radial direction. Coulomb friction force is taken into account in numerical analysis for roller bearings, which are modeled by

**Fig. 3** Analytical models of bearing supports**Fig. 4** Analytical model of cable restrainers

using the bilinear rectangle displacement-load relationship, shown in Fig. 3-b.

The continuous section (S2) in SB is supported on four pier units (P2, P3, P4 and P5) by steel bearings. Steel fixed bearing at top of P2 and steel roller bearings at top of P3, P4 and P5. On the other hand, the isolated continuous section (S2) in LRB is supported on four pier units (P2, P3, P4 and P5) by LRB. The left end is resting on the same P2 that supports S1, and at the right end on top of P5. Orientation of LRBs is such as to allow for longitudinal and transverse movements. LRB supports are represented by the bilinear force-displacement hysteresis loop presented in Fig. 3-c.

The principal parameters that characterize the analytical model are the pre-yield stiffness  $K_1$ , corresponding to combined stiffness of the rubber bearing and the lead core, the stiffness of the rubber  $K_2$  and the yield force of the lead core  $F_l$ . The structural properties of LRB supports are shown in Table 2. The devices are designed for optimum yield force level to superstructure weight ratio ( $F_l/W = 0.1$ ) and pre-yield to post-yield stiffness ratio ( $K_1/K_2 = 10.0$ ), which provide maximum seismic energy dissipation capacity as well as limited displacements<sup>4)</sup>.

It is also noted that properties of LRBs have been selected depending on the differences in dead load supported from the superstructure. The objective is to attract the appropriate proportion of non-seismic and seismic loads according to the resistance capacity of each substructure ensuring a near equal distribution of ductility demands over all piers. Furthermore, displacements of LRB have been partially limited for all the viaducts, through the installation of lateral side stoppers.

According to recommendations of Specifications for Highway Bridges in Japan, the pre-yield to post-yield stiffness ratio ( $K_1/K_2$ ) of the LRB is preselected to ensure a moderate period shift. Characteristics of isolation bearings are selected to obtain periods slightly larger than twice the fundamental period of the bridge when no isolation is applied (around 0.6 seconds in all cases). For the isolated models, the fundamental natural periods correspond to the modal shape in the longitudinal direction of the bridge, and the values in all isolated cases are about 1.3 seconds.

### 2.3 Expansion Joint

The isolated and non-isolated sections of the viaduct are separated, introducing a gap equal to the width of the expansion joint opening between adjacent spans in order to allow for contraction and expansion of the road deck from creep, shrinkage, temperature fluctuations and traffic without generating constraint forces in the structure. In the event of strong earthquakes, the expansion joint gap of 0.1m could be closed resulting in collision between deck superstructures.

The pounding phenomenon is modeled using impact spring elements for which the compression-only bilinear gap element is provided with a spring of stiffness  $K_i = 980.0 \text{ MN/m}$  that acts when the gap between the girders is completely closed.

On the other hand, in the analysis of the restrained models, in order to prevent excessive opening of the expansion joint gap, it is provided additional fail-safe protection against extreme seismic loads; for this purpose, unseating cable restrainers units are anchored to the three girder ends (1 unit per girder)

connecting both adjacent superstructures across the expansion joint.

Cable restrainers are relatively simple structures. Previous research on cable restrainer performance and design has included laboratory testing of cable restrainers<sup>5)</sup> and evaluation and development of design procedures<sup>6-11)</sup>. Post-earthquake evaluations from the 1989 Loma Prieta and the 1994 Northridge Earthquakes have shown that many cable restrainers were observed to have worked effectively during the earthquakes<sup>12)</sup>, preventing simply-supported spans from falling from their supports. However, the collapse of bridges such as the Gavin Canyon undercrossing and the Route 14/5 separation during the 1994 Northridge Earthquake proved that inadequate restrainer design can have catastrophic results<sup>13)</sup>. Large seismic forces are likely to cause either the cables to break or the bridge diaphragm walls at the two ends of the cables to suffer a punch-through action during a severe earthquake

The seismic restrainers, illustrated in Fig. 4, have been modeled as tension-only spring elements provided with a slack of 0.025 m, a value fitted to accommodate the expected deck thermal movements limiting the activation of the system specifically for earthquake loading. Initially, restrainers behave elastically with stiffness  $K_1$ , while their plasticity is introduced by the yield force ( $F_1$ ) and the post-yielding stiffness ( $K_2 = 0.05K_1$ ). Finally, the failure statement is taken into account for ultimate strength  $F_2$ , and since then, adjacent spans can separate freely without any action of the unseating prevention device. The structural properties of cable restrainer are presented in Table 3<sup>14)</sup>.

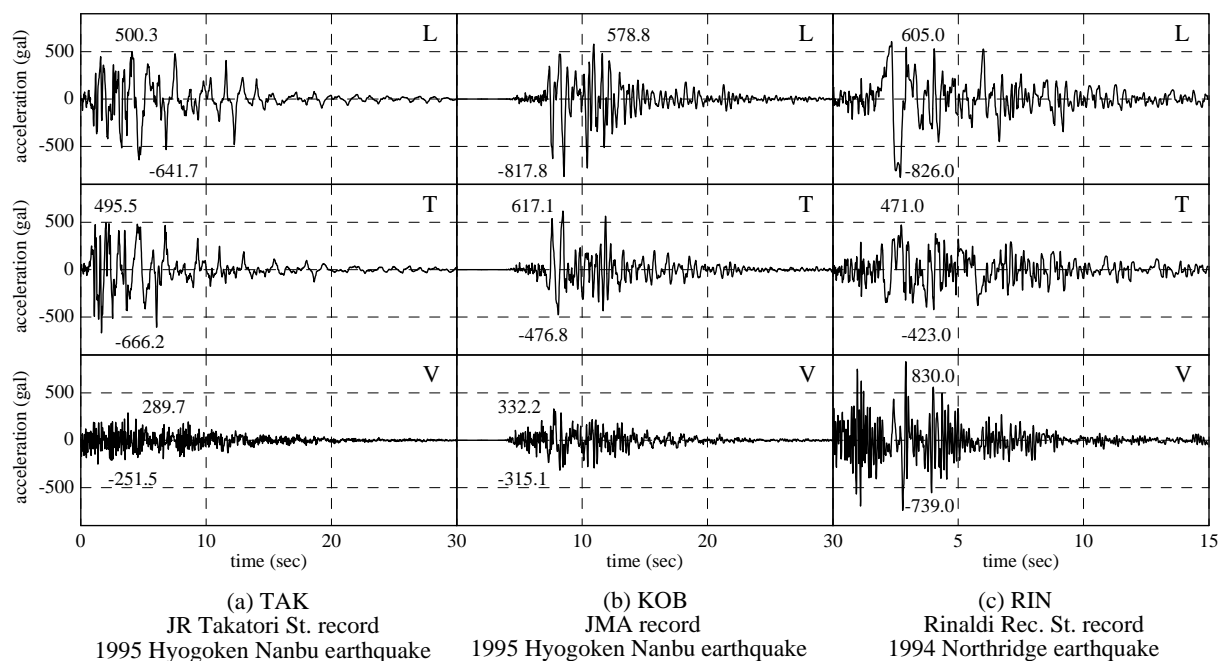


Fig. 5 Input earthquake ground motions

**Table 3** Structural properties of cable restrainers

|       | Units                               | Value   |
|-------|-------------------------------------|---------|
| $E$   | (Gpa)                               | 200     |
| $A$   | $\ast 10^{-3} \text{ (m}^2\text{)}$ | 1.765   |
| $L$   | (m)                                 | 1.730   |
| $K_1$ | (MN/m)                              | 204.058 |
| $K_2$ | (MN/m)                              | 10.203  |
| $F_1$ | (MN)                                | 2.584   |
| $F_2$ | (MN)                                | 3.040   |

### 3. METHOD OF ANALYSIS

The bridge model is developed in-house using the Fortran programming language. The analysis on the highway bridge model is conducted using an analytical method based on the elasto-plastic finite displacement dynamic response analysis. The governing nonlinear equation of motion can be derived by the principle of energy that the external work is absorbed by the work of internal, inertial and damping forces for any small admissible motion that satisfies compatibility and essential boundary conditions<sup>15</sup>. Hence, the incremental finite element dynamic equilibrium equation at time  $t+\Delta t$  over all the elements, can be expressed in the following matrix form:

$$[\mathbf{M}]\{\ddot{u}\}^{t+\Delta t} + [\mathbf{C}]\{\dot{u}\}^{t+\Delta t} + [\mathbf{K}]\{\Delta u\}^{t+\Delta t} = -[\mathbf{M}]\{\ddot{z}\}^{t+\Delta t} \quad (1)$$

where  $[\mathbf{M}]$ ,  $[\mathbf{C}]$  and  $[\mathbf{K}]^{t+\Delta t}$  represent respectively the mass, damping and tangent stiffness matrices of the bridge structure at time  $t + \Delta t$ . While  $\ddot{u}$ ,  $\dot{u}$ ,  $\Delta u$  and  $\ddot{z}$  denote the structural accelerations, velocities, incremental displacements and earthquake accelerations at time  $t+\Delta t$ , respectively. The incremental equation of motion accounts for both geometrical and material nonlinearities. Material nonlinearity is introduced through the bilinear elastic-plastic stress-strain relationship of the beam-column element, incorporating a uniaxial yield criterion and kinematic strain-hardening rule. The yield stress is 235.4 MPa, the elastic modulus is 200 GPa and the strain hardening in plastic area is 0.01.

Newmark's step-by-step method of constant acceleration is formulated for the integration of equation of motion. Newmark's integration parameters ( $\beta=1/4$ ,  $\gamma=1/2$ ) are selected to give the required integration stability and optimal result accuracy. The equation of motion is solved for the incremental displacement using the Newton-Raphson iteration scheme where the stiffness matrix is updated at each increment to consider geometrical and material nonlinearities and to speed to convergence rate. The damping mechanism is introduced in the analysis through the Rayleigh damping matrix, expressed as a linear combination of the mass matrix and the stiffness matrix.

The particular values of damping coefficients are set to ensure a relative damping value of 2% in the first two natural modes of the structure.

To assess the seismic performance of the viaduct, the nonlinear bridge model is subjected to the longitudinal (L), transverse (T), and vertical (V) components of three strong ground motion records (Fig. 5) from the Takatori (TAK) and Kobe (KOB) Stations during the 1995 Kobe Earthquake, as well as Rinaldi (RIN) Station, from the Northridge Earthquake in 1994.

The longitudinal earthquake component shakes the highway viaduct parallel to the X-axis of the global coordinate system, while the transverse and vertical components are acting in the Y- and Z-axes, respectively. The large magnitude records from the 1995 Kobe Earthquake and Northridge Earthquake used in this study, classified as near-fault motions, are characterized by the presence of high peak accelerations and strong velocity pulses with a long period component as well as large ground displacements<sup>16</sup>.

### 4. NUMERICAL RESULTS

The overall three-dimensional seismic responses of the viaducts are investigated in detail through non-linear dynamic response analysis. Particular emphasis has been focused on the expansion joint behavior due to the extreme complexity associated with connection between isolated and non-isolated sections in curved viaducts. The bridge seismic performance has been evaluated on four different radii of curvature, 100m, 200m, 400m, and 800m, considering two cases: viaducts with and without unseating cable restrainers.

In the analysis of the restrained models, in order to prevent excessive opening of the expansion joint gap, unseating cable restrainers units are anchored to the three girder ends (one unit per girder) connecting both adjacent superstructures across the expansion joint. The seismic restrainers, illustrated in Fig. 4, have been modeled as tension-only spring elements provided with a slack of 0.025m, a value fitted to accommodate the expected deck thermal movements limiting the activation of the system specifically for earthquake loading.

#### 4.1 Bearing Supports

Firstly, the effect of curvature radius on deck unseating damage is analyzed. During an earthquake, adjacent spans can vibrate out-of-phase, resulting in relative displacements at expansion joints. In simply-supported spans, the induced relative displacements to steel roller bearings can exceed the seat width at the pier top, causing the dislodgment of the rollers from the bearing assembly and the subsequent collapse due to deck superstructure unseating. The maximum roller bearing displacement in the negative tangential direction has been established as the damage index to evaluate the potential

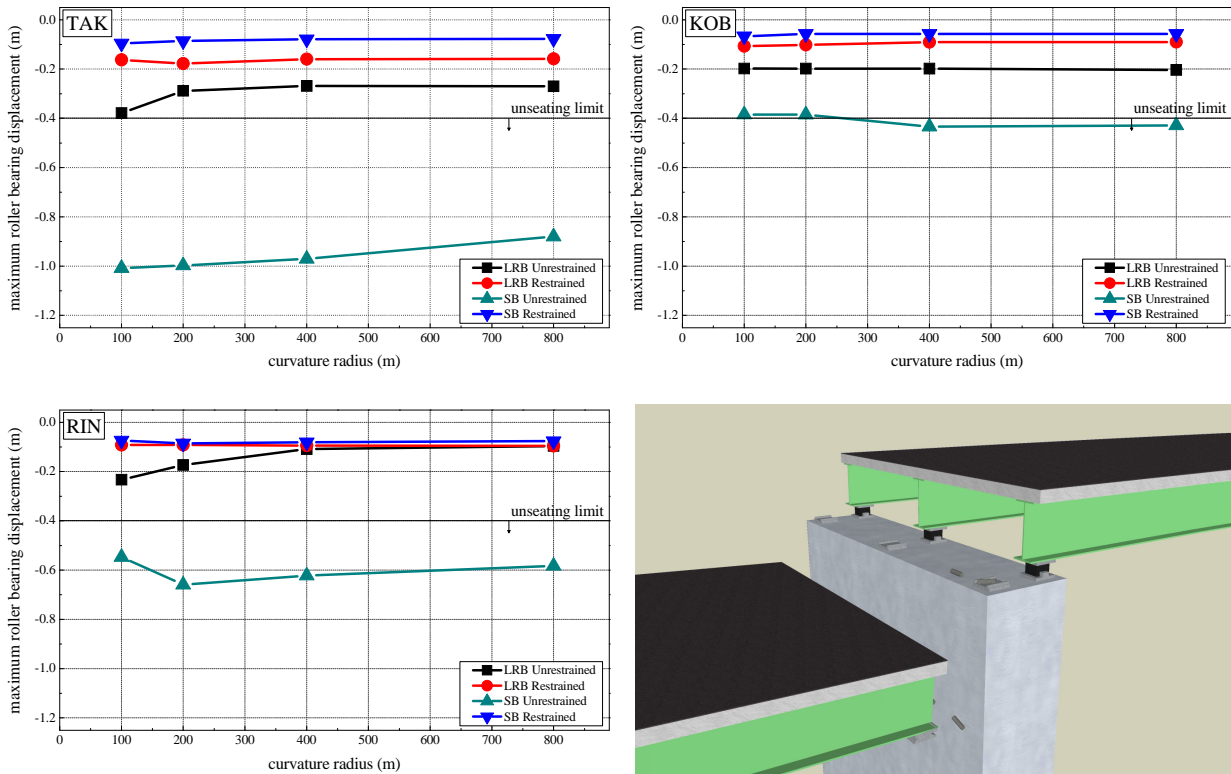


**Fig. 6** Curvature effect on deck unseating damage

possibility of deck unseating. For this study, a limit of 0.40 m has been fixed to determine the high unseating probability for existing bridges with narrow steel pier caps that provide short seat widths.

First, the unrestrained viaducts are analyzed in terms of the maximum displacement on the steel roller bearing. The results, shown in Fig. 6, indicate that most of the viaducts supported on steel bearings and subjected to the three earthquake inputs clearly overpass the unseating limit, being only 100m and 200m viaducts in KOB the exceptions. It can be observed that TAK represents the worst condition for all the curvatures. In the same way, the response obtained from RIN shows extremely high displacements. KOB presents smaller values; however those are still close or even over the unseating limit for the bridges with 400m and 800m curvature radius. It can be noticed the excessive vulnerability to unseating damage of curved viaducts equipped with steel bearings. The response of the viaducts equipped with LRB supports is also shown in Fig. 6. It can be observed that once the continuous section has been isolated, its seismic response improves significantly in all the curvatures. However, even though the values are remarkable smaller than those from the steel cases, there is still a clear effect of the curvature radius in terms of maximum roller bearing displacements on TAK and RIN inputs.

For restrained viaducts, similar values of maximum displacements on the roller bearing are observed in both, steel and LRB viaducts. Both cases present a remarkable reduction

on the maximum displacements in comparison with the obtained in the unrestrained cases; particularly in the bridges with 100m curvature radius. From the results, it can be observed that the input record representing the worst scenario is TAK input, producing significantly higher displacements that put in risk the superstructure of the viaducts.

#### 4.2 Expansion Joint Damage

Permanent tangential offsets at expansion joints cause, in several cases, traffic closure and the disruption of the bridge usability in the aftermath of the earthquakes resulted in a critical problem for rescue activities. This residual joint separation is mainly attributed to the final position of roller bearings relative to the supported superstructure. The relative inclination between adjacent piers, caused by the fact that seismic damages at the bottom of piers are not identical, has been also considered as an additional source of residual opening. The residual joint tangential displacement has been calculated in order to perform the post-earthquake serviceability evaluation on the viaduct. The possibility for vehicles to pass over the tangential gap length, measured as the contact length of a truck tire (0.15 m), is suggested as the limit for this damage. For unrestrained bridges supported on steel bearings, as shown in Fig. 7, the results of the residual joint tangential displacement show unacceptable residual displacements at the expansion joint when subjected to TAK and RIN, most of the bridges overpass the separation limit, while KOB input represents less severe damage. It can be seen

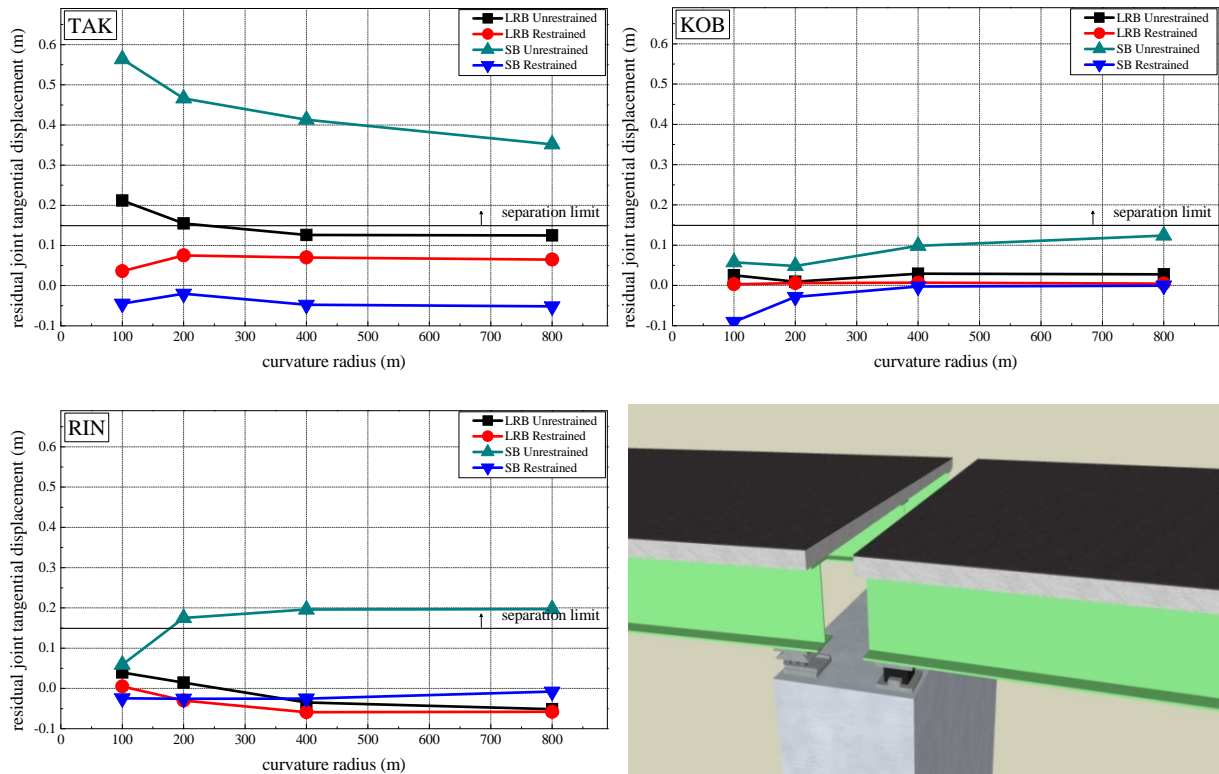


**Fig. 7** Curvature effect on tangential joint residual damage

that TAK produce the most severe condition for the structures, while the other inputs still remain close to the limit. TAK input represents an important damage in the bridge with 100m and 200m curvature radii in both cases, steel and LRB supports viaducts. In this response, the separation limit has been overpassed, causing by this the disruption of the bridge serviceability.

In the viaducts equipped with the LRBs, KOB and RIN do not represent significant risk. Regarding the differences on the bearing supports, there is a critical disadvantage in terms of residual displacements presented at the viaducts with steel bearings. The bridges with LRB supports present an important reduction on the possibility of seismic damage. However, even with the use of LRB supports, the bridges with 100m and 200m curvature radii still remain over the separation limit. It is observed that as the curvature radius increases, the behavior of the bridges tends to be less severe.

The results obtained from the analysis of the restrained viaducts are also shown in Fig. 7. The application of cable restrainers produces an important variation on the behavior of the bridges in comparison with the cases of unrestrained bridges. This effect is extensive for steel and LRB supports viaducts in all inputs. Firstly, a significant reduction in the tangential offsets of expansion joints is observed. For none of the bridges equipped with unseating prevention systems the separation limit of 0.15m is exceeded. In all the viaducts the residual

displacement is observed under 0.08m. Clearly, the use of unseating prevention systems not only provides a residual displacement lower than the separation limit but also maintains these limits in similar values.

Another important problem presented in the expansion joint during the earthquake is the pounding damage. While seismic isolation provided by LRBs beneficially reduces the transmitted forces into the piers, the important added flexibility results in detrimental increase of collisions between adjacent decks. Due to this pounding phenomenon a remarkable point to note is that, in addition to the expected local damage at colliding girders, high impact forces are transmitted to bearing supports located in the proximity of the expansion joint<sup>17</sup>.

The large spikes analytically observed in both, tangential and radial, components of reaction forces make the steel bearing supports particularly vulnerable to failure, which could result into the collapse of the bridge. Ratios of maximum impact force to the deck weight greater than 1.0 have been observed to provide a good estimation of significant transmitted forces to bearing supports<sup>18, 19</sup>. Therefore, the analytical response of curved viaducts in terms of pounding damage is studied.

The analytical results for the unrestrained viaducts, as illustrated in Fig. 8, show that the higher values of impact forces are presented in the viaduct with steel bearings and curvature radius of 100m, followed by the bridge with 200m of curvature radius.

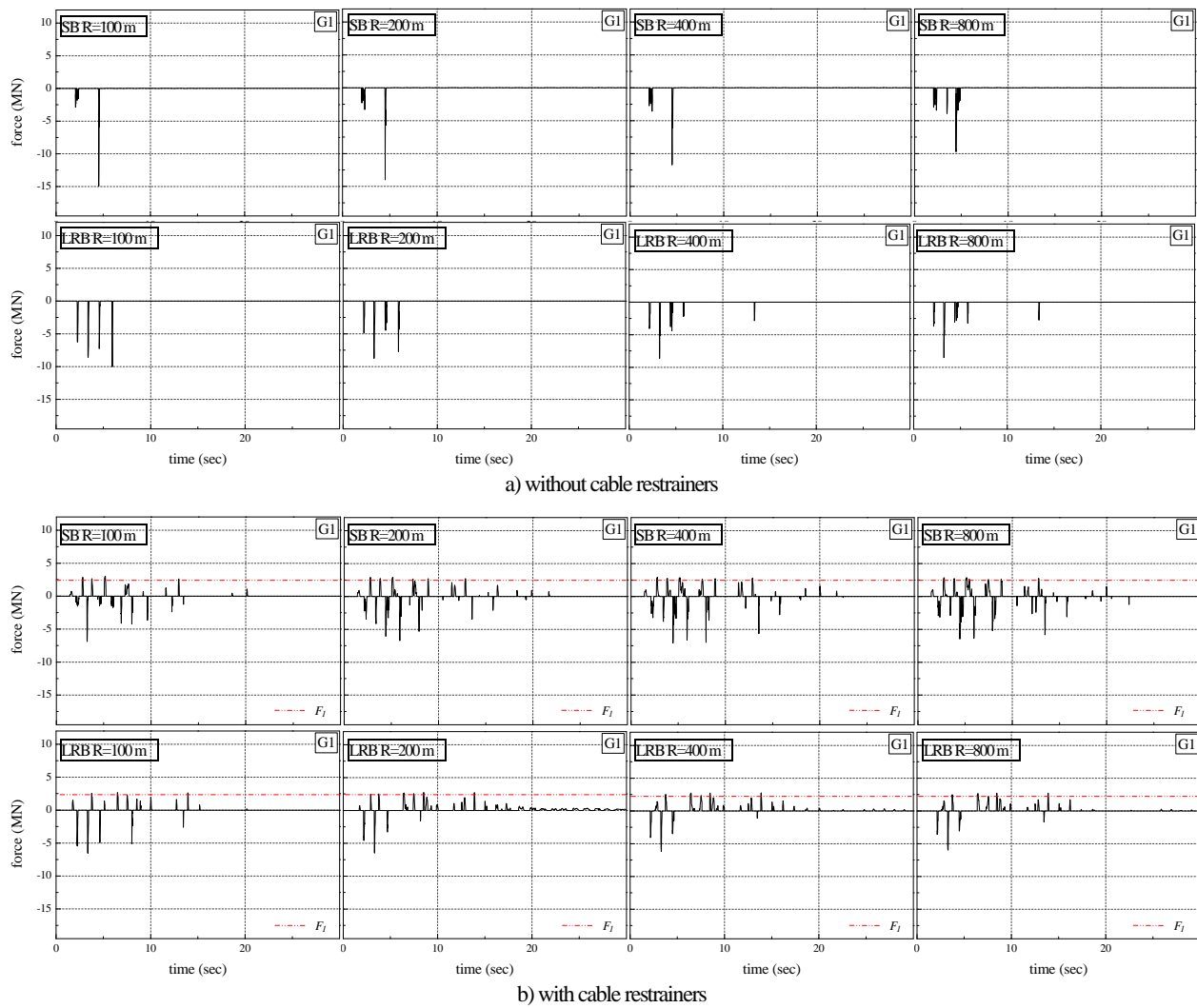


**Fig. 8** Maximum Impact forces at expansion joint from TAK

The last two viaducts with 400m and 800m of curvature radii have impact forces slightly less severe in most of the cases. It can be noticed the extremely high impact forces presented in the more curved viaducts with steel bearings as well as in the cases with LRB supports. In the worst condition, viaduct with 100m and steel bearings, the maximum values reach 15 MN, while the 100m viaduct equipped with LRB supports reach just 10 MN. Fig. 8 shows the results from TAK, which represents the most severe condition. For the viaducts equipped with cable restrainers, the reduction in the possibility of pounding damage is significant. Firstly, the use of restrainers reduces the impact forces in all viaducts, despite the curvature radius and the differences on bearing supports; this can be noticed even in the bridge with radius of curvature of 100m. This effect applies as well to the other bridges with 200m, 400m and 800m of curvature radii, as presented in Fig. 8. In the results from the restrained viaducts, it is still possible to observe the advantages of replacing the steel bearings for LRBs. The use of seismic isolation devices reduces the possibility of excessive impacts at the expansion joint. Such results prove the effectiveness of the

combination of seismic isolation devices and unseating prevention system. Furthermore, it is possible to observe the remarkable advantages of the use of a deck unseating prevention system based on cable restrainers, especially in terms of pounding damage at the expansion joint. The results indicate that the installation of cable restrainers effectively reduces the relative displacements at the expansion joint, and therefore the possibility of pounding damage.

### 4.3 Pier at Expansion Joint

First, for unrestrained viaducts, the seismic response in terms of displacements at the top of the piers with steel bearings is analyzed. For TAK input, which is the worst condition for the viaducts, the results show excessive displacements at the top of P2. Fig. 9 shows the pier top displacements trajectories observed at top of the pier supporting the expansion joint. It can be observed the high values reached by the viaducts with no seismic isolation and no cable restrainers. For the viaducts where LRBs have been installed, the seismic response presents a remarkable reduction on the displacements at top of the piers.



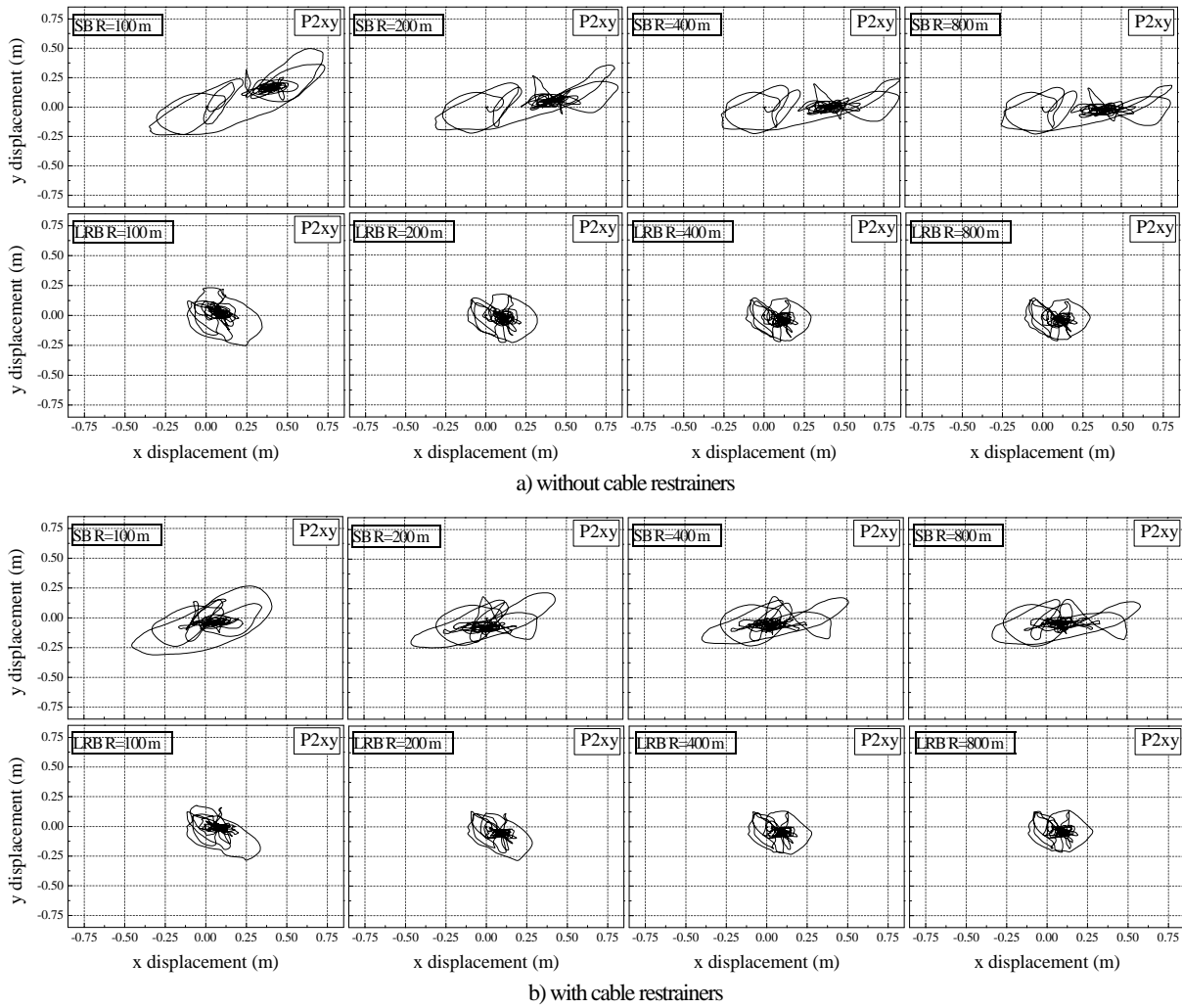


**Fig. 9** Pier top displacement trajectories at P2 from TAK input

It can be easily noticed the effectiveness of the use of LRB supports in order to reduce the seismic damage presented at top of the P2. However, it can be observed that even after the installation of LRBs, it is still possible to observe the effects of the curvature radius on the displacements at top of the piers, especially in the viaduct with 100m radius. The results obtained from the restrained viaducts are also shown in Fig. 9. The installation of cable restrainers effectively reduces the displacements at top of P2 in both cases, viaducts with steel bearings and with LRBs. However the displacements observed in the viaducts supported on steel bearings still present excessive displacements. On the other hand, the viaducts supported on LRBs show an important reduction on the displacements, not only from the ones obtained in the steel bearing case but also from the ones observed in the viaducts with no cable restrainers.

## 5. CONCLUSIONS

The effectiveness of seismic isolation in order to reduce the possibility of seismic damage on curved highway viaducts has been analyzed. The three-dimensional nonlinear seismic

dynamic response has been evaluated. Moreover, the effectiveness of cable restrainers to mitigate earthquake damage through connection between isolated and non-isolated sections of curved steel viaducts is evaluated. The investigation results provide sufficient evidence for the following conclusions:

The calculated results clearly demonstrate that curved viaducts are more vulnerable to deck unseating damage. It has been observed that for more curved viaducts, this possibility increase significantly. However, this type of seismic damage is reduced initially by the installation of LRBs and subsequently by the installation of cable restrainers. Moreover, the use of cable restrainers provides to the bridge a similar behavior in case of curved and straight tending bridges, despite of the curvature radii. In terms of tangential joint residual damage, curved viaducts are found particularly vulnerable. This damage was significantly reduced once LRBs were installed. In restrained viaducts, an important reduction of the residual joint tangential displacement is appreciated and similar values of residual joint tangential displacement are obtained.

Also curved viaducts are found vulnerable to pounding damage. Viaducts supported on steel bearings represent the

worst conditions in terms of seismic response, while seismically isolated cases prove to be more effective. A significant reduction in the impact forces at the expansion joint is observed by the installation of LRB supports. Furthermore, even though the differences on the radii of curvature among the viaducts, the application of cable restrainers reduces the possibility of pounding damage. Finally, in this analysis, the effectiveness of seismic isolation combined with the use of cable restrainers on curved highway viaducts is demonstrated, not only by reducing in all cases the possible damage but also by providing a similar behavior in the viaducts despite of curvature radius.

## References

- 1) Japan Road Association (JRA), *Specifications for Highway Bridges – Part V Seismic Design*, Maruzen, Tokyo, 2002.
- 2) Robinson, W. H., Lead-rubber hysteretic bearings suitable for protecting structures during earthquakes, *Earthquake Engineering Structures*, Vol. 10, pp. 593-604, 1982.
- 3) Maleki, S., Effect of deck and support stiffness on seismic response of slab-girder bridges, *Engineering Structures*, Vol. 24, No. 2, pp. 219-226, 2002.
- 4) Mendez Galindo C., Hayashikawa T., Ruiz Julian F.D., Effects of curvature radius on nonlinear seismic response of curved highway viaducts equipped with unseating prevention cable restrainers, *Journal of Constructional Steel*, JSSC, Vol. 14, pp. 91-98, 2006.
- 5) DesRoches, R., Pfeifer, T., Leon, R. T., and Lam, T.: Full-scale tests of seismic cable restrainer retrofits for simply supported bridges, *Journal of Bridge Engineering* ASCE, Vol. 8, No. 4, pp. 191-198, 2003.
- 6) Saiidi, M., Maragakis, E.A., and Feng, S.: An evaluation of the current Caltrans seismic restrainer design method, *Rep. No. CCEER-92-8*, Civil Engineering Department, University of Nevada, Reno, 1992.
- 7) Saiidi, M., Maragakis, E., and Feng, S.: Parameters in bridge restrainer design for seismic retrofit, *Journal of Structural Engineering* ASCE, Vol. 122, No. 1, pp. 61-68, 1996.
- 8) Fenves, G., and DesRoches, R.: Response of the Northwest Connector in the Landers and Big Bear earthquakes, *Rep. No. UCB/EERC-94/12*, Earthquake Engineering Research Center, University of California, Berkeley, 1994.
- 9) Yang, Y. S., Priestley, M.J. N., and Ricles, J. M.: Longitudinal seismic response of bridge frames connected by restrainers, *Rep. No. SSRP-94/09*, Structural System Research, University of California, San Diego, 1994.
- 10) Trochalakis, P., Eberhard, M.O., and Stanton, J. F.: Evaluation and design of seismic restrainers for in-span hinges, *Rep. No. WA-RD 387.1*, Washington State Transportation Center, Seattle, 1995.
- 11) Priestley, M. J. N., Seible, F., and Calvi, M.: Seismic design and retrofit of bridges, Wiley, New York, 1996.
- 12) Yashinsky, M.: Chapter 30: Earthquake damage to structures. In: Chen, W. F., editor. *Structural Engineering Handbook*, Boca Raton, CRC Press, 1999.
- 13) Duan, L., and Chen, W. F.: Chapter 18: Bridges. In: Chen, W. F., and Scawthorn, C., editors. *Earthquake Engineering Handbook*, Boca Raton, CRC Press, 1999.
- 14) Takeno, S., Ohno, H., and Izuno, K.: Velocity-based design of seismic unseating prevention cable and shock absorber for bridges, *Structural Engineering and Earthquake Engineering*, Vol. 21, No. 2, pp. 175-188, 2004.
- 15) Ali HM, Abdel-Ghaffar AM. Modeling the nonlinear seismic behavior of cable-stayed bridges with passive control bearings. *Computer & Structures*, Vol. 54, No.3, pp. 461-92, 1995.
- 16) Somerville P.G., Magnitude scaling of the near fault rupture directivity pulse. *Physics of the Earth and Planetary Interiors*, Vol. 137, pp. 201-12, 2003.
- 17) Zhu P., Abe M., Fujino Y., Evaluation of pounding countermeasures and serviceability of elevated bridges during seismic excitation using 3D modeling. *Earthquake Engineering & Structural Dynamics*, Vol.33, No.5, pp.591-609, 2004.
- 18) Mendez Galindo C., Hayashikawa T., Ruiz Julian F.D., Pounding and deck unseating damage of curved highway viaducts with piers of unequal heights, *Journal of Constructional Steel*, JSSC, Vol. 15, pp. 285-292, 2007.
- 19) Kawashima, K., and Shoji, G.: Effect of restrainers to mitigate pounding between adjacent decks subjected to a strong ground motion, *12<sup>th</sup> World Conference on Earthquake Engineering*, Paper No. 1435, 2000.

(Received September 18, 2008)